Iranian Journal of Chemistry and Chemical Engineering (IJCCE)

Investigation of the Effect of Silver Nanoparticles Obtained from *Primula Vulgaris* Extracts by Applying the Green Synthesis Method on MCF-7 Cells

Harun Ciftci [a,b],

[a]Department of Medical Biochemistry, Faculty of Medicine, Kırşehir Ahi Evran University, Kırşehir, TURKEY

[b]Cankiri Karatekin University Rectorate, Çankırı, TURKEY,

harunciftci@yahoo.com

Cigdem Er Caliskan* [c],

[c*]Department of Field Crops, Faculty of Agriculture, Kırşehir Ahi Evran University, Kırşehir, TURKEY, cigdemer86@gmail.com

Burcu Yazici [d],

[d]Department of Molecular Medicine, Institute of Health Sciences, Kırşehir Ahi Evran University, Kırşehir, TURKEY burcumutluyazici@gmail.com

Akin Tekcan [e],

[e]Department of Medical Biology, Faculty of Medicine, Amasya University, Amasya, TURKEY

akin.tekcan @amasya.edu.tr

Kubra Ozturk [f]

[f] Department of Genetics and Bioengineering, Faculty of Engineering and Architecture, Kırşehir Ahi Evran University, Kırşehir, TURKEY

kubraademirbag@gmail.com

[1]*To whom correspondence should be addressed.

+E-mail: cigdemer86@gmail.com & cigdem.ercaliskan@ahievran.edu.tr

ABSTRACT:

In recent years, the use of nanoparticles has gained significant attention in cancer research due to their unique properties and potential as targeted drug delivery systems. This study focuses on the synthesis and characterization of Primula vulgaris stabilized silver nanoparticles (PVAgNPs) and the evaluation of in vitro cytotoxicity against MCF-7 cells. In this study, PVAgNPs were synthesized separately from the flower ($PVAgNPs_F$), leaf ($PVAgNPs_L$), and root ($PVAgNPs_R$) extracts of Primula vulgaris (PV). The PVAgNPs were characterized by various analytical techniques, including UV-Visible absorption spectroscopy, Fourier transform infrared spectroscopy (FTIR), X-ray diffraction, dynamic light scattering (DLS), zeta potential, and scanning electron microscopy (SEM). The maximum absorption wavelengths are obtained at 437 nm for the $PVAgNPs_R$ samples and at 440 nm for the $PVAgNPs_F$ and $PVAgNPs_L$ samples. Based on the XRD spectra, PVAgNPs were found to have a cubic crystal structure. On average, the zeta potential values of PVAgNPs ranged from -14 to -28 mV, indicating that they were quite stable. SEM analysis showed that the synthesized PVAgNPs were predominantly spherical in shape and ranged in size from 40 to 89 nm. The iCELLigence Real-Time Cell Analysis (RTCA) system was used to evaluate the efficacy of the synthesized PVAgNPs against MCF-7 cell lines. After 24 h of incubation, the inhibitory concentrations (IC_{50}) of $PVAgNPs_L$ $PVAgNPs_R$, and $PVAgNPs_F$ were determined to be 30.37, 36.74, and 57.64 µg/mL, respectively, indicating that PVAgNPs have an in vitro cytotoxic effect on MCF-7 cells. In conclusion, the synthesis of PVAgNPs was successfully achieved using a green synthesis approach. In addition, a thorough characterization of these nanoparticles was carried out, confirming their structural properties, and demonstrating their efficacy against MCF-7 cell lines. These results highlight the potential of PVAgNPs as promising candidates for the development of novel anticancer drugs. However, further studies are required to evaluate their feasibility and efficacy for future therapeutic applications.

KEYWORDS: *Silver Nanoparticles, Green Synthesis, Primula vulgaris, Cytotoxic effects, MCF-7.*

INTRODUCTION

Cancer is a major global health problem with a significant impact on morbidity and mortality [1]. Among cancers affecting women, breast cancer takes the lead, constituting approximately 30% of all female cancer cases. In addition, breast cancer has the second highest mortality rate in women after lung cancer [2]. Therefore, it is critical to develop effective and advanced therapies to reduce the impact of this disease. Many studies in this field show that unwanted side effects can be reduced by adopting a targeted approach [3]. Nanoparticles are attracting increasing interest in cancer treatment due to their special physical and chemical properties, leading to the emergence of a new field of cancer treatment called cancer nanomedicine [3, 4]. Compared to conventional anticancer agents, metallic nanoparticles (MNPs) can be used as novel therapeutic agents or drug carriers along with drug candidates [5]. Nanomedicine investigates the applicability of nanotechnological information and tools for the prevention, treatment, diagnosis, and control of diseases [6]. In this context, among various types of metallic nanoparticles (Pd, Cu, Au, Zn, Sn, and Co) ranging from 1 to 100 nm in diameter, silver nanowires/nanoparticles (AgNPs) stand out as particularly remarkable. AgNPs possess attractive physicochemical properties and biological functionalities [7], such as high antimicrobial activity [8], and show lower toxicity to cells compared to other metallic nanoparticles [6, 9]. They also exhibit a broad spectrum of bactericidal properties [10], anticancer properties [11], and other therapeutic capabilities. Moreover, AgNPs have the ability to form various nanostructures [12] and relatively low production costs [6, 13]. These properties make AgNPs one of the most attractive nanomaterials. Nanoparticles can be synthesized using a variety of methods, which include chemical, physical, and biological techniques [14, 15]. However, most traditional methods involve the use of toxic chemicals and generate waste, causing environmental pollution [16]. In contrast, biological synthesis, also known as green synthesis, offers advantages such as low cost, renewability, environmental friendliness, and ease of application [17-19]. Extracts from different parts of plants (leaves, stems, roots, shoots, flowers, bark, and seeds) are used for the synthesis of AgNPs of different sizes and shapes [20]. These plant extracts contain various organic components such as enzymes, alcohols, flavonoids, alkaloids, quinines, oils, terpenoids, and phenolic compounds [21]. These organic compounds have different functional groups such as hydroxyl, carbonyl, and amidogen [22] which contribute to the reduction of Ag^{+} to Ag^{0} [3]. In addition, plant derivatives contain various natural substances, including starch, cellulose, chitin, dextran, and alginates, which can act as reducing agents and stabilizers in nanoparticle synthesis [3]. Medicinal plants, containing numerous phytochemicals with high therapeutic value and devoid of toxic chemicals, also serve as natural coating agents [23]. AgNPs have shown promise as anticancer agents due to their potent anticancer properties and extremely low toxicity [24]. Many studies have reported favorable results in the use of AgNPs in various types of cancer, including breast cancer [25, 26], cervical cancer [27], colon cancer [26], ovarian cancer [28], pancreatic ductal adenocarcinoma [29] and lung cancer [30]. Furthermore, studies have shown that AgNPs have a strong effect on MCF-7 cell line compared to other cell lines [19, 31].

Primula vulgaris (PV) used in the study is a perennial flowering plant commonly known as 'primrose' and belongs to the *Primulaceae* family [32]. Primrose species are predominantly found in the Northern Hemisphere and grow naturally in temperate regions of Europe, South America, Asia, and North Africa [33]. The leaves and petals are edible [34]. The roots of PV are known for their expectorant, diuretic, antispasmodic, and analgesic

properties [35]. The flowers of this plant are also rich in various organic compounds. Özkan et al. reported that presence of various phenolic compounds (gallic acid, protocatechuic acid, p-hydroxy benzoic acid, catechin, vanillic acid, caffeic acid, syringic acid, epicatechin, p-coumaric acid, ferulic acid, rutin, trans-cinnamic acid, and luteolin) in *PV.* [36]. This indicates that *Primula* species are a potential source for the synthesis of AgNPs. However, no study has been reported on the synthesis of silver NPs from PV extract and the evaluation of their cytotoxic properties. In this study, a green synthesis pathway using extracts of PV flowers ($PVAgNPs_F$), leaves ($PVAgNPs_L$) and roots ($PVAgNPs_R$) was employed for the synthesis of silver nanoparticles. The synthesized AgNPs can adsorb many organic compounds due to their large surface area [37, 38]. Therefore, the porous AgNPs formed because of the reduction process adsorb various organic molecules from the mixture of PV extract and appear as PVAgNP. Additionally, the *in vitro* cytotoxic effects of these synthesized silver nanoparticles on MCF-7 breast cancer cell lines were investigated.

MATERIAL AND METHODS

Materials

All reagents used in this study were of analytical grade. Aqueous solutions were prepared using ultrapure water obtained from a Milli-Q water purification system (Millipore Corporation, MA, USA). Silver nitrate salt ($AgNO_3$) was purchased from Merck, Germany. Commercial silver nanoparticles (CAgNP) with particle sizes ranging from 48 nm to 78 nm were purchased from Nanografi, USA. MCF-7 cell line was obtained in the 14th passage from Baskent University, Faculty of Medicine, Department of Medical Biology, Ankara, Turkey. Cisplatin solution (50 mg/100 mL) was purchased from Kocak, Turkey. The plant material (PV) was collected from Salıpazarı (Samsun), Turkey (latitude 41° 4' 50" N, longitude 36° 49' 36" E) in May 2019.

Preparation of the Primula Vulgaris Extract (PVE)

The identification of the leaf, root, and flower of the PV samples was carried out by Dr. Ekrem Aktoklu, plant systematics expert at Kırşehir Ahi Evran University, Kırşehir, Turkey. The samples were washed with water on the same day. They were then dried in an oven at 50°C for 24 h and powdered using a mechanical muller. 10.0 g of powdered plants were boiled in 100 mL of pure water for 15 min, rested for 15 min, and filtered through Whatman Grade No. 1 filter paper (11 µm) and used for further studies [39].

Lyophilization of Plant Extract (LPE)

100 mL of PVE were transferred to Falcon tubes and centrifuged at 4500 rpm for 1 h using a Beckman Coulter Microfuge 20R. After centrifugation, the liquid in the Falcon tubes was discarded and the wet solid sample collected at the bottom of the tube was transferred to Eppendorf tubes. After the lyophilization process, the LPE samples were obtained as solids (Labconco, Freezone Plus).

Synthesis of Primula vulgaris Silver Nanoparticles (PVAgNPs)

10 mL of PVE (from leaf, flower, and root separately) were gradually added to 90 mL $AgNO_3$ solutions of different concentrations (10^{-4} to 10^{-2} mol/L). The samples were then kept in the dark (25 °C) for 24 h. The colourless $AgNO_3$ solution was converted into a dark brown colour which indicated the reduction of Ag^+ to Ag^0. Subsequently, the synthesized PVAgNPs were collected from the solution through centrifugation at a speed of 4500 rpm for 60 minutes at a temperature of 4°C. The resulting PVAgNPs were then subjected to a drying process at lyophilizer until they reached a powdered form, for both characterization and cytotoxicity studies. Fig. 1 shows a schematic of the synthesis of Ag-NPs.

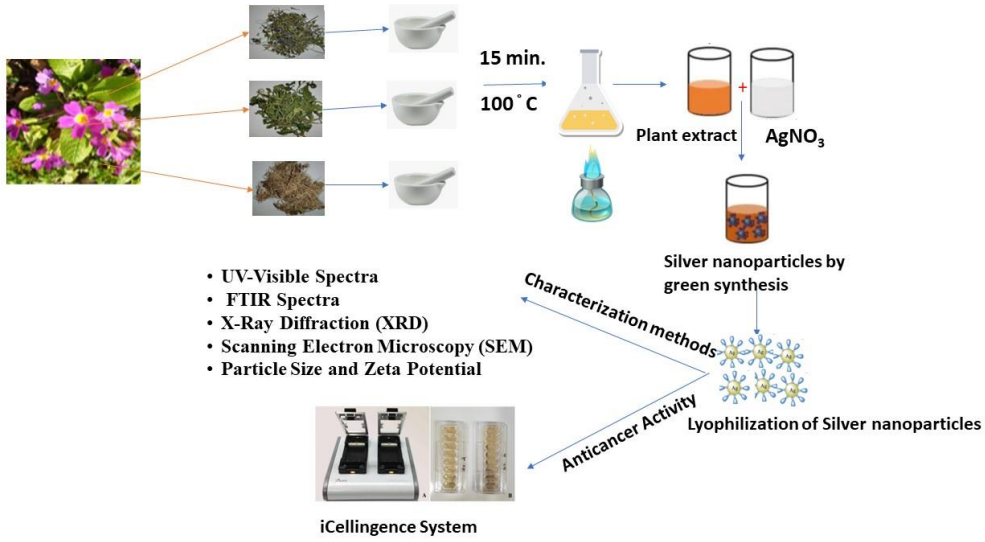

Fig. 1: Synthesis of Ag-NPs using PV (leaf, root, and flower) extract.

UV-Visible Spectra Analysis

UV-Visible spectroscopy was used as a preliminary test to determine the formation of silver NPs. The spectroscopic analyzes were performed at Kırıkkale University KÜBTUAM Center in Kırıkkale, Turkey. A volume of 1.0 mL of the synthesized PVAgNP solutions were collected and measured with a UV-Visible spectrophotometer (Perkin Elmer, Lambda 35) at wavelengths between 300 and 700 nm.

FTIR Analysis

Fourier transform infrared spectroscopy (FTIR) is a measurement method used to determine the structure and properties of-functional groups-based on the wavelength of light [40]. In this study, FT-IR analysis (Thermo Scientific, Nicolet 6700) was performed at the AHİ laboratory of Kırşehir Ahi Evran University in Kırşehir, Turkey. The samples were ground with KBr pellets and measured in FTIR spectrum in the range of 4000-400 cm^{-1}.

XRD Analysis

X-ray diffraction (XRD) is a method used to obtain information about the elemental composition or crystallographic structure of naturally and artificially synthesized NPs [41]. The XRD analysis (PANanalytical, Empyrean) was performed at Bozok University, Yozgat, Turkey. It was analyzed with the XRD instrument with a step size of 0.02 between 10° and 90° in the 2θ range.

Scanning Electron Microscopy (SEM)

SEM is an imaging technique that determines the size, surface, and shape morphology through direct visualization of NPs [42]. SEM images (FESEM/Carl Zeiss Sigma 300 VP) were obtained from Çankırı Karatekin University, Çankırı, Turkey. The samples were coated with gold before analysis, the accelerating voltage was 5 kV and the films were examined at 50.00KX magnification.

Particle Size and Zeta Potential

Dynamic Light Scattering (DLS) was used for particle size analysis of PVAgNPs. Zeta potential is defined as the electrical potential in the slip plane [43]. DLS analysis was performed at Çankırı Karatekin University using Malvern/Zetasizer, Nano ZS ZEN3600 brand device, and zeta potential analysis was performed at Kırıkkale University using Malvern/Zetasizer, Nano ZSP brand device.

Cell Culture

The iCELLigence real-time cell analysis system (RTCA) was used to determine the cytotoxic effects and IC_{50} doses of PVAgNPs on MCF-7 cell lines. In the RTCA system, 2 system-specific E-plates containing 8 wells were used. PVAgNPs were applied when the cell index values reached the desired level at the end of 24 h on the E-plates and left for incubation at 37°C in 5% CO_2 environment. For cell culture studies, 25 mg of the $PVAgNPs_F$, $PVAgNPs_L$, and $PVAgNPs_R$ were weighed, added to volumetric flasks, and the final volume was completed to 50 mL with pure water. Thus, PVAgNPs solutions were obtained at a concentration of 500 µg/mL. Different doses (12.50 to 100 µg/mL) were used from the 500 µg/mL solution. They were applied to the cells in 2 repetitions. Final volumes were completed to 600 µL with cell medium. After the extracts were applied, cytotoxic measurements were made with the iCelligence device every 15 min, and real-time cell viability analyzes were performed for 96 h. The results obtained were evaluated based on cell index values in RTCA Data Analysis Software 1.0. After the application of PVAgNPs, time-dependent impedance values and cell index values (IC_{50}: dose value that inhibits half of the cells) were obtained at 24 and 48 h. To observe the normal cell growth curve, 2 wells were created without any extract applied, and only MCF-7 cells were cultivated.

RESULTS AND DISCUSSION

Synthesis of AgNPs from $AgNO_3$ using plant extracts is one of the most popular methods for the synthesis of silver colloids. The ability of PV leaf, root, and flower extracts to reduce silver ions to AgNPs was confirmed by the reddish-brown color change of the reaction mixture. This is because, in the case of Ag-NPs, the excitation of surface plasmon resonance typically results in a reddish-brown color [44].

UV-Visible light spectroscopy is used to evaluate the formation of AgNPs by measuring the optical absorption spectra. The UV-Visible spectra ranging from 300 to 600 nm of the $PVAgNPs_F$, $PVAgNPs_L$, and $PVAgNPs_R$ samples, are shown in Fig. 2. The maximum absorption wavelengths are obtained at 437 nm for the $PVAgNPs_R$ samples and at 440 nm for the $PVAgNPs_F$ and $PVAgNPs_L$ samples (Fig. 2). Fig. 2 shows an increase in the absorbance of $PVAgNPs_{F\text{-}L\text{-}R}$. The reason for this increase is that the concentration of reducing agent required to reduce silver ions to silver decreased in roots, flowers, and leaves [45].

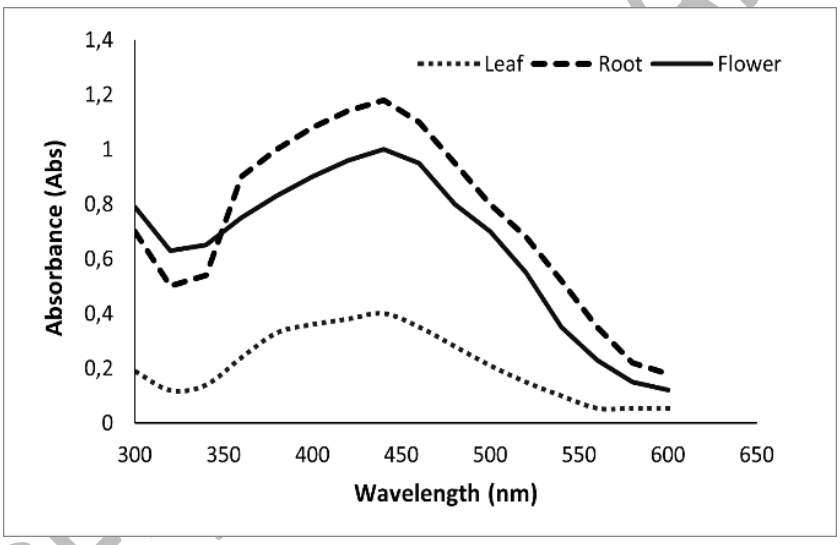

Fig. 2: UV-Visible spectra for PVAgNPs.

The evaluation of AgNPs formation using a UV-Visible spectrophotometer is a very important technique. It has been reported that strong and large surface plasmon absorption peaks were observed in the formation of various metal NPs of 2-100 nm size in different studies [46, 47]. Kelkawi et al. have found the wavelength of maximum absorption for synthesized AgNPs using *Mentha pulegium* extracts as 450 nm [48]. In another study, Jang et al. found the wavelength of maximum absorption for synthesized AgNPs using extracts of *Lonicera hypoglauca* flower as 437 nm [49]. The peak around 400 nm is attributed to surface plasmon resonance (SPR), which is due to collective oscillations of the electron conduction band of the AgNPs [50].

The concentration of $AgNO_3$ was varied in the range of 10^{-4} to 10^{-2} mol/L, to observe its effect on the size and morphology of the synthesised AgNPs. 90 mL $AgNO_3$ was gradually added to 10 mL aqueous extracts of flowers,

leaves and roots. After 24 h, lyophilized PVAgNPs were measured by UV spectroscopy at 440 nm. The absorbance value increases as the concentration of silver nitrate solution increases. This indicates that the amount of silver NPs increases with the increasing concentration. When the concentration reaches 10^{-3} mol/L, the absorbance becomes maximum, indicating that the maximum amount of nanosilver particles are formed under the synthesis conditions. A partial decrease at higher concentrations indicates the decrease in the formation of AgNPs due to the depletion of the PVE reducing agent. Therefore, 10^{-3} mol/L silver nitrate solution was considered sufficient for 10 mL PVE. FT-IR investigations revealed the presence of different biomolecules in the extract of PV that could be involved in the reduction of metal salt. The FTIR spectrum of as-prepared LPE and PVAgNPs is shown in Fig. 3. By studying the spectra, it was possible to identify and analyze the functional groups present in the samples, which provided valuable information about the chemical composition and properties of the materials.

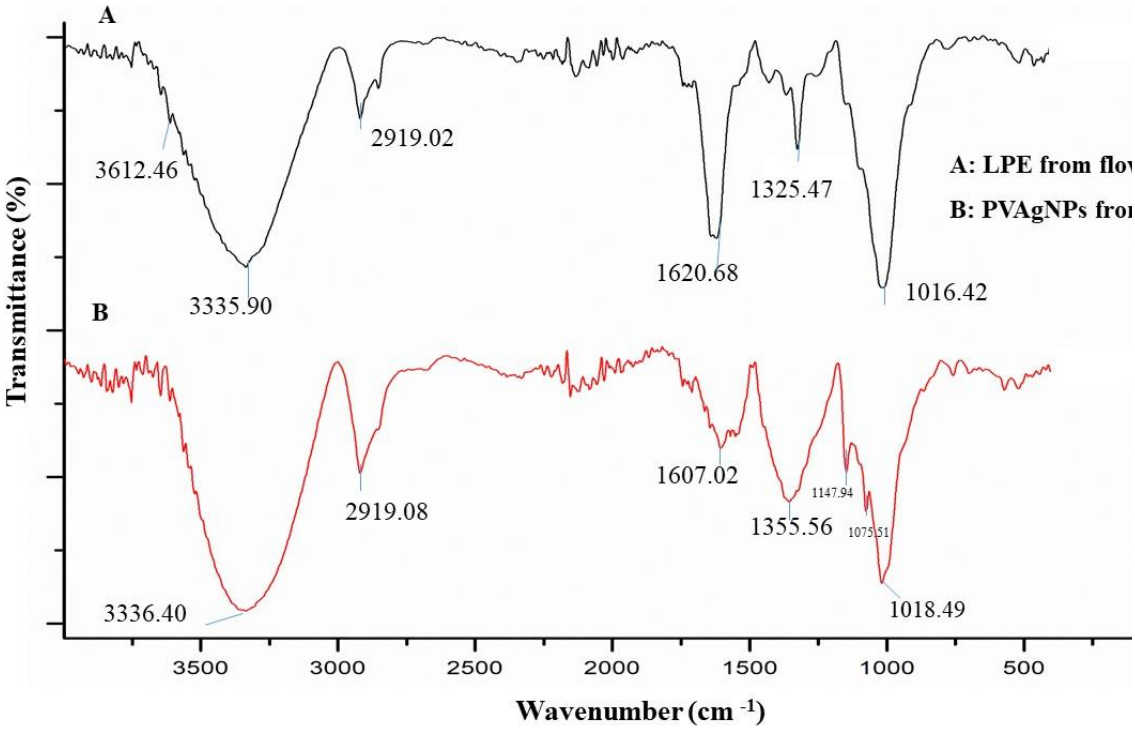

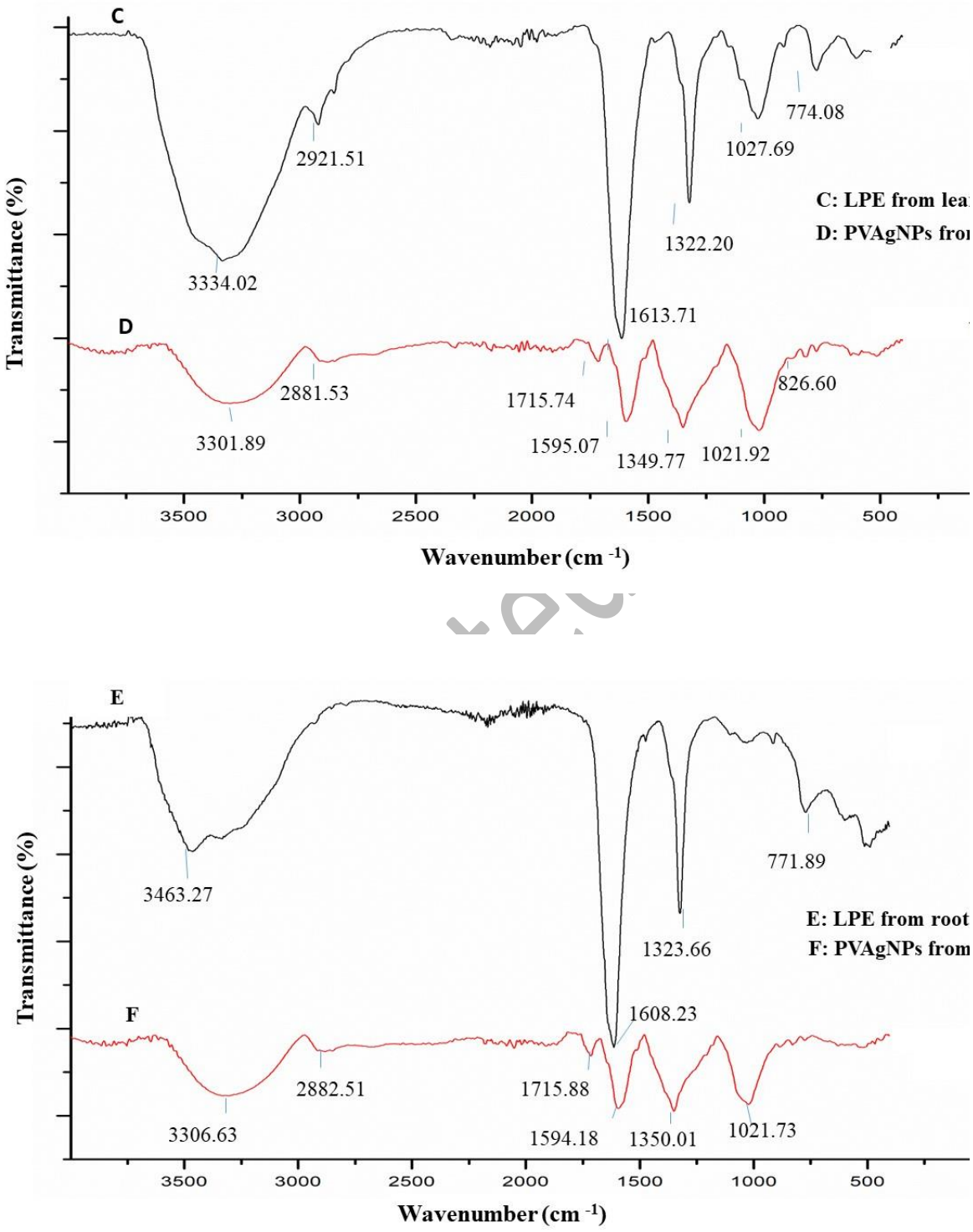

Fig. 3: FT-IR spectra of LPEs and PVAgNPs (A: LPE from flower, B: PVAgNPs$_F$, C: LPE from leaf, D: PVAgNPs$_L$, E: LPE from root, F: P PVAgNPs$_R$).

According to the FT-IR measurement results, the peak values of functional groups present in prepared from different parts of PVAgNPs were: 3301, 2881, 1715, 1595, 1349, 1021 and 826 cm^{-1} for $PVAgNPs_L$; 3306, 2882, 1715, 1594, 1350 and 1021 cm^{-1} for $PVAgNPs_R$; 3336, 2919, 1607, 1355, 1147, 1075 and 1018 cm^{-1} for $PVAgNPs_F$. The bands around 3300-3400 cm^{-1} in the spectra of PVAgNPs correspond to O-H stretching vibrations, indicating the presence of alcohol and phenol. Peaks in the range of 2935 and 2880 cm^{-1} are related to the stretching vibrations of C-H. In the IR spectra, bands around 1610 cm^{-1} correspond to C=N vibrations, and bands in the range of 1476-1437 cm^{-1} and around 1320 cm^{-1} correspond to N-H and C=C stretching vibrations, respectively. The bands at ~ 1017 cm^{-1} to 1022 cm^{-1} are characteristic of the C-O stretching vibration in carbohydrates, while the band at ~ 825 cm^{-1} is generally characteristic of the bending vibration of the C=O bond in carbohydrates and was found in all NP samples. The band ~~found on~~ at ~ 1021 cm^{-1} indicates carboxylic acid, ester, and ether groups of proteins and metabolites that may be involved in the synthesis of nanoparticles [51]. The band observed around ~1600 cm^{-1} in all nanoparticles indicates the existence of flavonoids, according to our findings [52]. In the spectra, the peaks revealed at 1027 and 774 cm^{-1} are attributed to the C-O and C-C single-bond stretching vibrations. The strong bands at 2919 cm^{-1} of CH_3 stretch of alkane/carboxylic acids were present in $PVAgNPs_F$ and were absent in and $PVAgNPs_R$. Some changes were observed in the IR spectra of PVAgNPs samples compared to LPE. The peaks in A shifted from 1620 and 1325 cm^{-1} to 1607 and 1355 cm^{-1}, peaks in C shifted from 3334, 1613, 1322, and 1027 cm^{-1} to 3301, 1595, 1349, and 1021 cm^{-1}, and peaks in E shifted from 3463, 1608.23, and 1323 cm^{-1} to 3306, 1594.18, and 1350 cm^{-1}. The shift of the peaks was due to the interaction of PVEs with silver ions from silver nitrate as well as the effect of other compounds present in the extracts.

Studies show that Primula species are rich in saponins, alkaloids, tannins, terpenes, and phenolic compounds [36, 53], which is consistent with the presence of flavonoids and phenolic compounds in the AgNP we synthesized. While the FT-IR spectrum doesn't provide a definitive depiction of the conjugated compounds' structure on the nanoparticle surface, it does indicate the presence of diverse functional groups within the sample [54]. Hydroxyl, carboxyl, phenolic, and amine groups in the plant were effective in reducing Ag^+ ions to Ag by forming bonds with metal and the formed AgNPs acted as a coating and stabilizing agent [55]. Therefore, it was concluded that phytochemicals and biomolecules present in the plant content play a dual role in the formation and stabilization of green synthesized AgNPs. These identified bands collectively affirm the participation of plant metabolites in the AgNPs synthesis process.

The presence of AgNPs in the synthesized product can be verified using the X-ray diffraction (XRD) technique. Confirmation was achieved by observing the characteristic peaks in the XRD spectrum that correspond to the face-centered cubic crystal structure of metallic silver. X-ray diffraction patterns of PVAgNPs were obtained in the 2θ = 20–80 angle range. XRD results are given in Fig. 4.

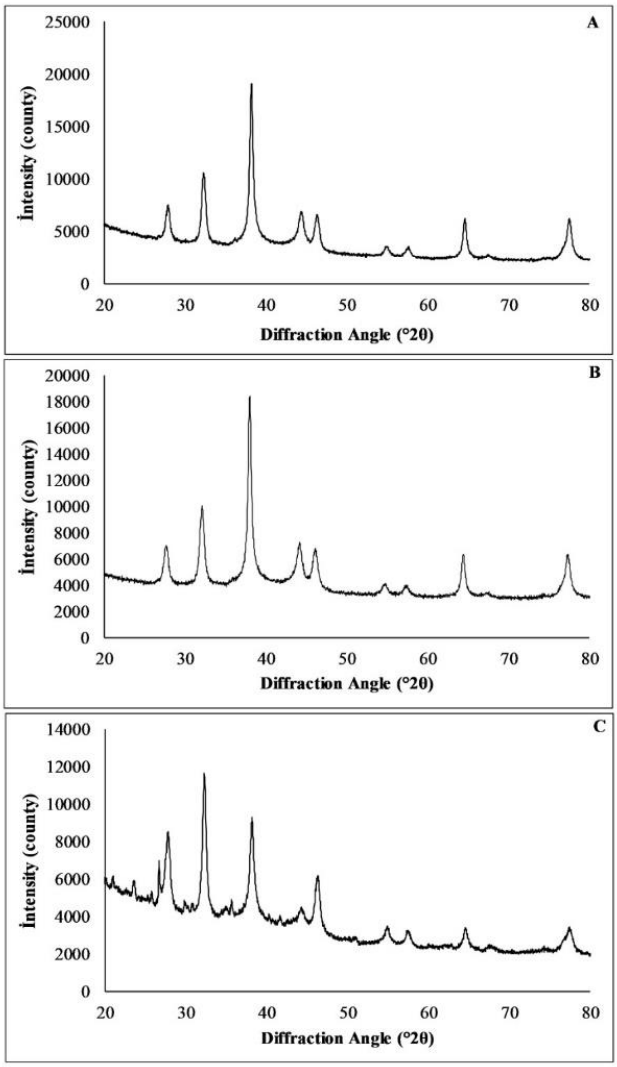

Fig. 4: XRD-spectra of PVAgNPs (A: PVAgNPs$_F$, B: PVAgNPs$_L$, C: PVAgNPs$_R$).

In this study, Ag (111) signals of PVAgNPs were detected around 38.15 degrees. Strong peaks were observed, indicating the high degree of crystallinity of biosynthesized Ag-NPs. It was determined that the face-centered cubic crystal structure of the synthesized AgNPs showed dense Bragg diffraction peaks at 38.15, 44.42, 64.80, and 77.72, corresponding to the values of the (111), (200), (220), and (311) lattice planes, respectively. The expansion of the Braggs peaks indicates the formation of NPs, and the resulting XRD patterns are consistent with previous studies [56].

These results are consistent with the Universal Joint Committee. Powder Diffraction Standard No. 04-0783 AgNPs and confirm the crystal shape [57]. The XRD spectrum results clearly show that the prepared AgNPs have crystallized. The high degree of crystallinity also indicates that the biosynthesized AgNPs have well-defined crystal structures, which is important for their stability and performance in various applications. These data led to the conclusion that silver NPs were successfully prepared using plant materials. *Ramar et al.* reported intense peak values, corresponding to Bragg reflection in XRD analysis of AgNP using *Solanum trilobatum* plant (111), (220),

and (311) [58]. *Vivek et al.* reported similar results in the XRD analysis of AgNP using *Annona squamosa* extract [59]. The literature has reported many similar studies [18, 60].

SEM images of synthesized PVAgNPs using green synthesis are given in Fig. 5. SEM images show that the particles have spherical structures, and their sizes vary in the range of 40 to 89 nm. The particle size distributions ranged from 40.2 nm to 78.7 nm for $PVAgNPs_L$, 41.1 nm to 74.9 nm for $PVAgNPs_F$, and 47.3 nm to 88.9 nm for $PVAgNPs_R$. Dhar et al. synthesized silver nanoparticles using *Phyllanthus emblica* fruit extract and silver nitrate. They reported that the synthesized silver nanoparticles had a spherical shape and the average grain size ranged between 60 and 80 nm [61]. In the study done by Logeswari *et al*. AgNPs were synthesized using *Ocimum tenuiflorum*, *Solanum trilobatum*, *Syzygium cumini*, *Centella asiatica,* and *Citrus sinensis* plant extracts and they reported that the sizes of the synthesized NPs by SEM images were found as 28 nm, 26.5 nm, 65 nm, 22.3 nm, and 28.4 nm, respectively [62]. Rani et al. synthesised AgNPs using *Cucumis melo* L. leaf extract. By SEM analysis, their structure and dimensions were found to be spherical and the observed range for AgNPs was 66.7 to 92.3 nm [63].

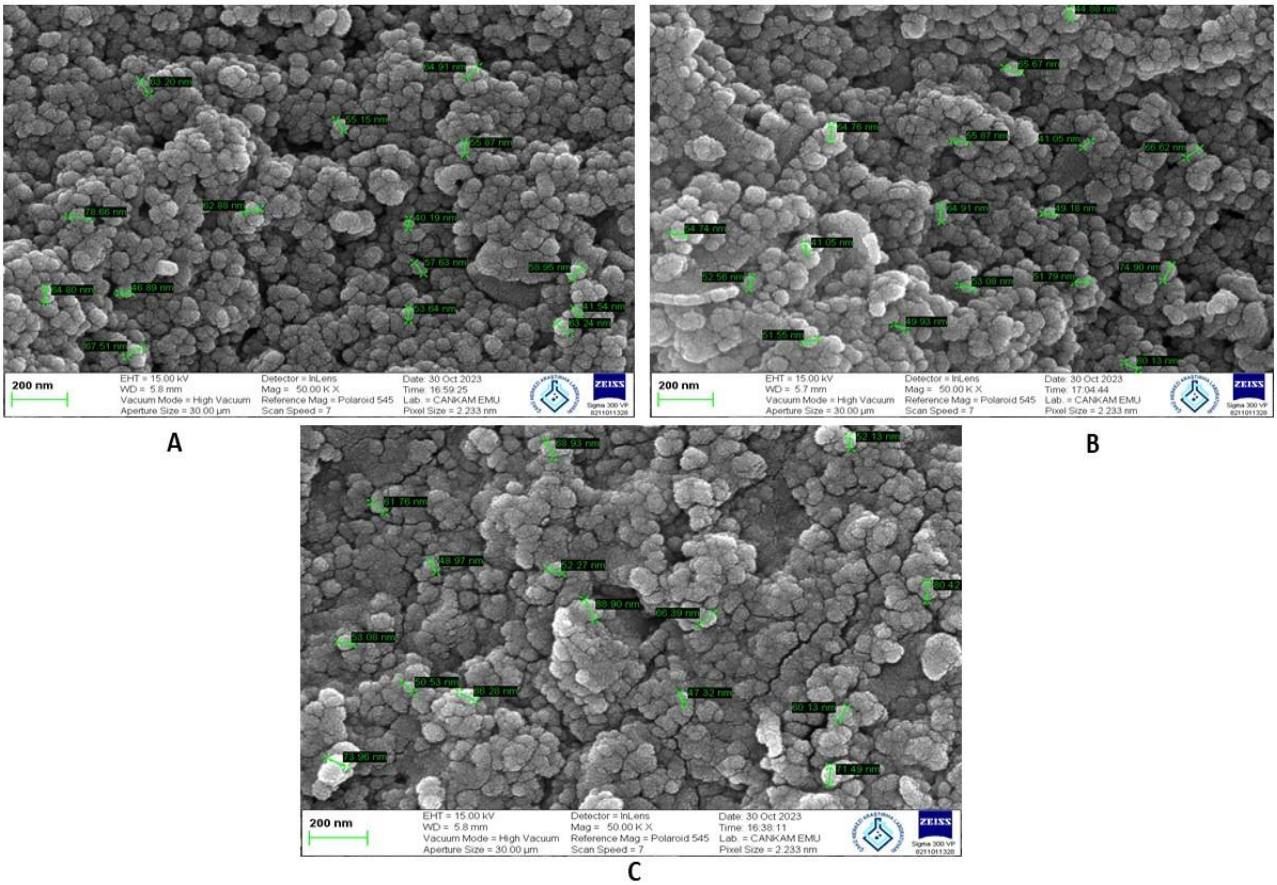

Fig. 5: SEM images of PVAgNPs (A: $PVAgNPs_F$, B: $PVAgNPs_L$, C: $PVAgNPs_R$).

Zeta potential is a parameter that measures electrostatic interactions between solid particles or liquid droplets in a dispersion (suspension or emulsion). In colloidal media, the attractive Van der Waals force between particles determines the way these units collide, merge or separate. Zeta potential analysis provides information on this subject. Zeta potential is the electrical potential in the plane of suspension. The change in environmental stress is a direct measure of the tendency to clump and separate. The measurement of zeta potential is critical for understanding dispersion and aggregation processes. The magnitude of the zeta potential stabilizes colloidal suspensions by preventing aggregate formation. The electrical charge zeta potential analysis of the synthesized PVAgNPs is shown in Fig.6.

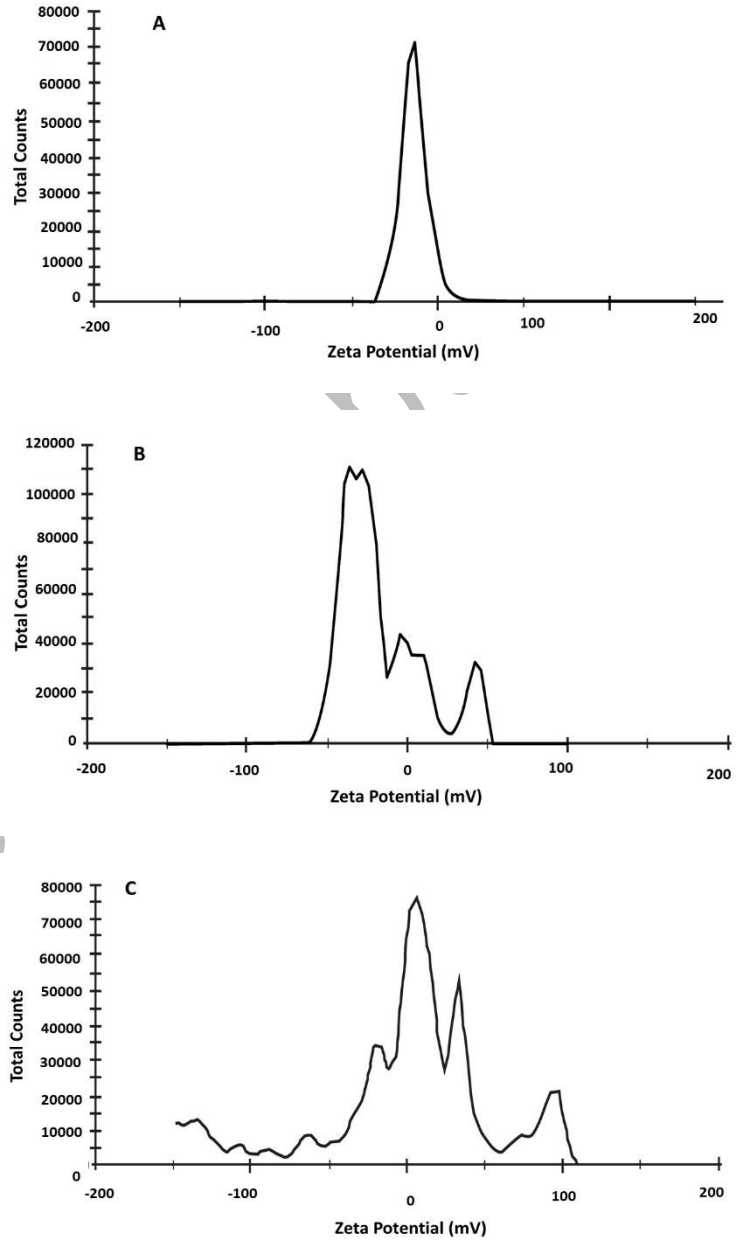

Fig. 6: Zeta Potentials of PVAgNPs (A: PVAgNPs$_F$, B: PVAgNPs$_L$, C: PVAgNPs$_R$).

The results showed that all the samples indicated were fairly stable, as the measured negative zeta-potential values showed, and the mean ranged from -14 to -28 mV. The mean standard deviation of the measurements in this stable region in the measurements is within ± 5 mV. Only at extreme dilutions has the value of the zeta potential changed and we call it an unstable region in the literature [64, 65].

DLS is a method used to analyze and determine the size and distribution of particles. It is particularly effective for measuring the size of AgNPs because it can accurately measure particles ranging from a few nanometers to a few microns. This technique works by analyzing the change in light frequency caused by interactions with particles of different sizes. Smaller particles cause a greater shift in light frequency [11, 66]. The particle size and size distribution of nanoparticles can be determined using many commercially available instruments. The instruments can be used to analyze dry powders and powders dispersed in suspension. Particle size scatter plots of PV samples show that particle sizes range from 63.7 to 140.3 nm. The mean particle size distribution of PVAgNPs was in the range of 63.7 nm for the leaf, 77.3 nm for the flower, and 140.3 nm for the root (Fig. 7).

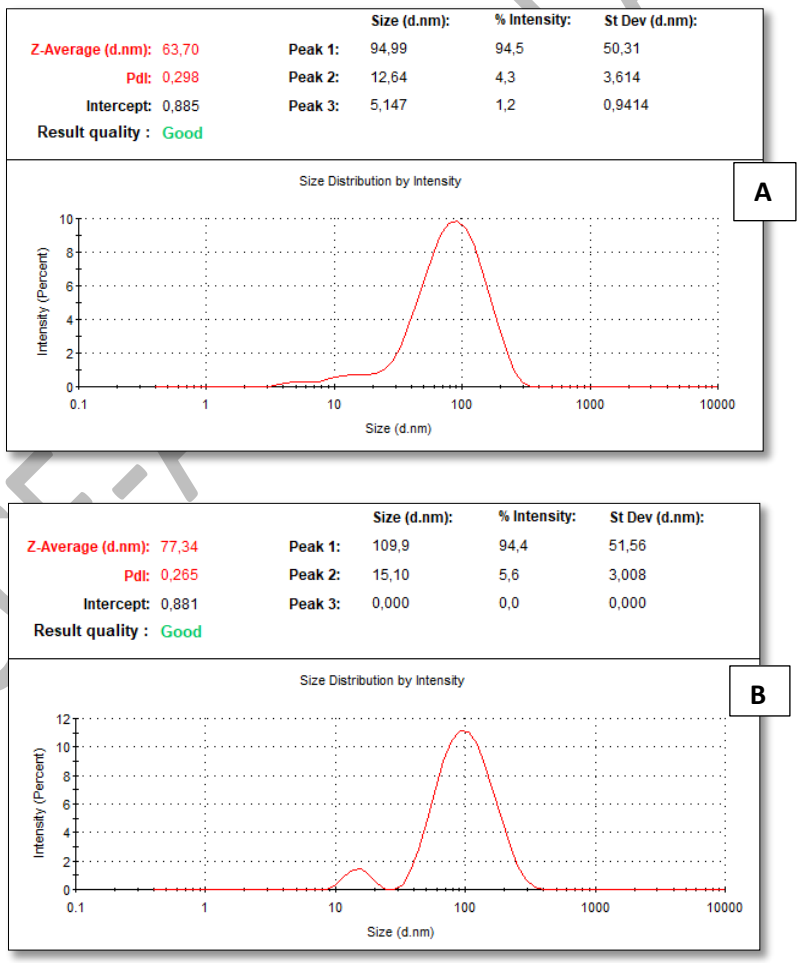

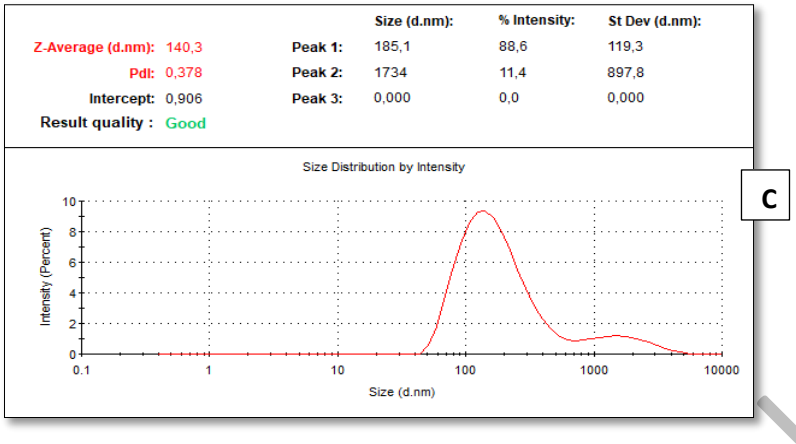

Fig.7: Particle size of PVAgNPs (A: PVAgNPs$_F$, B: PVAgNPs$_L$, C: PVAgNPs$_R$).

The in vitro cytotoxicity activities of AgNPs synthesized using simple and green method on MCF-7 cell lines were investigated. Fig. 8 the MCF-7 breast cancer cell lines, which were exposed to the PVAgNPs to evaluate cytotoxic effects.

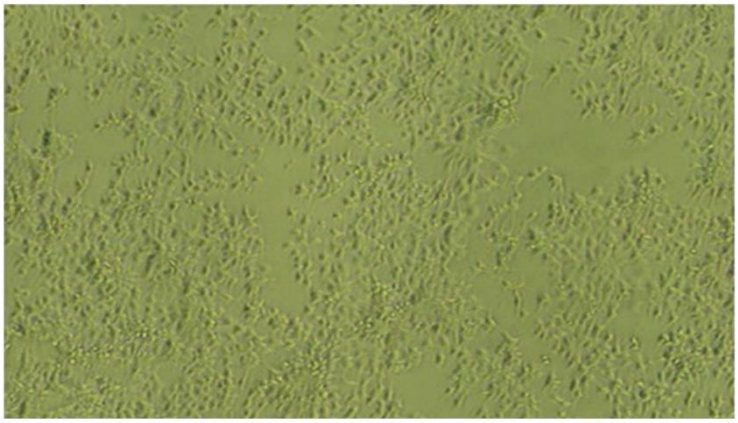

Fig 8: Microscopic view of MCF-7 breast cancer cell cultures.

The iCELLigence real-time cell analysis system (RTCA) assay was used to determine the cytotoxicity effects of the AgNPS and cisplatin used as a positive control in the range of 12.50 to 100 µg/mL. It was determined that the IC_{50} values 24 h after application of all doses were 36.74 µg/mL in the root, 30.37 µg/mL in the leaf, 57.64 µg/mL in the flower, and 41.01 µg/mL in the cisplatin (Fig. 9). The examination revealed that all three AgNs demonstrated effective antiproliferative performance within the MCF-7 cell line. This was evident as they induced a reduction in the growth curve rate based on the cell index (CI), correlating with an escalation in concentration in comparison to the control cells. Notably, PVAgNP$_L$ and PVAgNP$_R$ (at 30.37 and 36.74 µM, respectively) exhibited an IC_{50} value lower than that of cisplatin (at 40.01 µM) against MCF-7 human breast cancer cells. However, PVAgNP$_F$ displayed a higher IC_{50} value of 43.76 µM. It has been reported in the literature that because of the polyphenols, they contain, PV extracts exhibit selective cytotoxic effects against human A549, HepG2, MCF-7, prostate (PC-3), and colon (WiDr) cancer cell lines. Polyphenols are an important class of

secondary herbal metabolites reported to exhibit potent antioxidant properties [67]. In particular, recent studies have reported that polyphenols can inhibit the proliferation of cancer cells by activating cell cycle arrest, apoptosis, and cell signaling [68]. The leaves of PV have bioactive components such as apigenin, scopoletin, *p*-coumaric acid, rosmarinic acid, and ferulic acid, and their levels are higher than the flower and root samples [67-69]. There have also been considerable investigations on the anticancer properties of these compounds in various types of cancer cells [70, 71]. Therefore, the cytotoxic effect of AgNPs obtained from leaf extract is higher than that of AgNPs obtained from flowers and roots. Various studies have investigated the cytotoxic effects of different *Primula* species on cancer cell lines [67, 72, 73]. In a study investigating the effects of the extract obtained from the flowers of the PV plant using dimethyl sulfoxide on human colon (WiDr), lung (A549), liver (HepG2), breast (MCF-7), and prostate (PC-3) cancer cell lines; demonstrated that it exerts a selective cytotoxic effect on all cancer cell lines and determined an IC_{50} value of 191.8-375.3 µg/mL [73]. In another study, it was found that leaf extracts of the PV plant had cytotoxic effects on human lung (A549), liver (HepG2), breast (MCF-7), prostate (PC-3), and colon (WiDr) cancer cell lines compared to normal fibroblast cells demonstrated and found that the IC_{50} values ranged from 133.3-253.8 µg/mL in five cancer cell lines [67]. In this study, it was observed that PVAgNPs had a cytotoxic effect on MCF-7 cell lines. Considering the literature information, our findings on the proliferation profiles of PVAgNPs (leaf, root, and flower extract) on MCF-7 cell lines are consistent with previous studies. From this point of view, it is seen that PVAgNPs have antiproliferative effects on cancer cells.

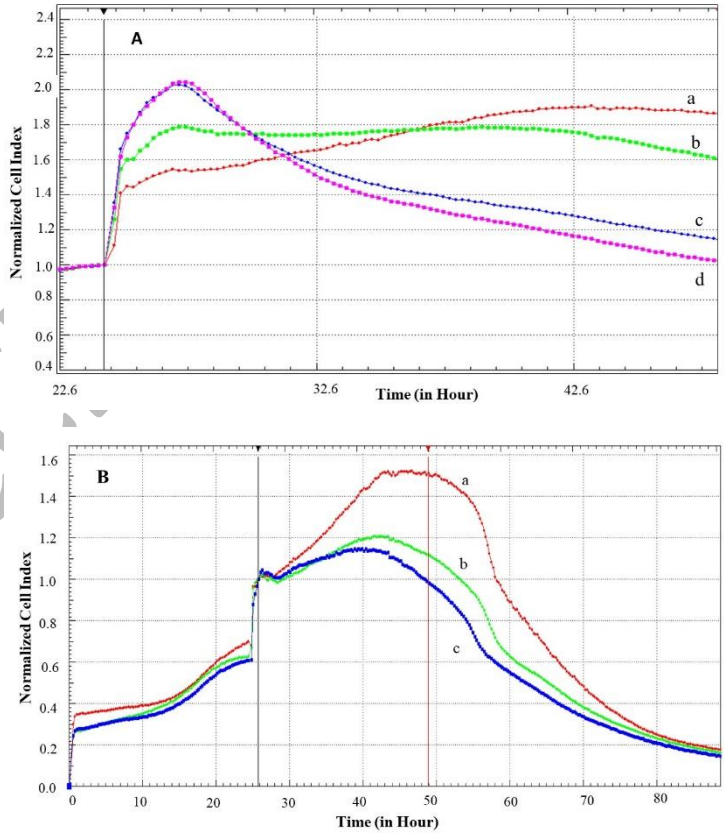

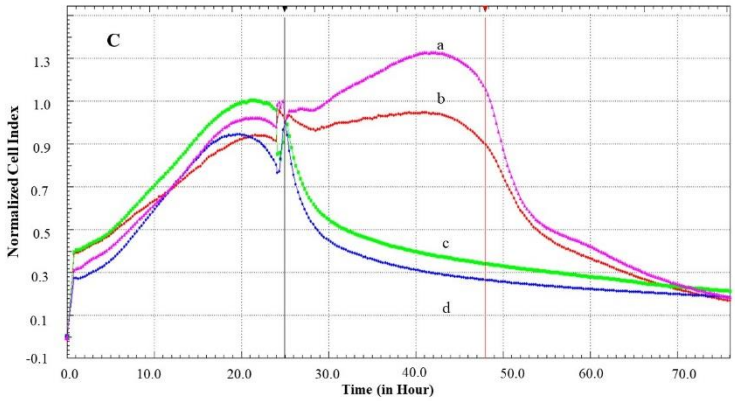

Fig. 9: Real-time cell analysis results for PVAgNPs in various doses.

(A: PVAgNPs$_F$, a: 25 µg/mL, b: 50 µg/mL, c: 75 µg/mL, d: 100 µg/mL. B: PVAgNPs$_R$, a: 25 µg/mL, b: 50 µg/mL, c: 100 µg/mL. C: PVAgNPs$_L$, a: 12.5 µg/mL, b: 25 µg/mL, c: 50 µg/mL, d: 75 µg/mL)

Studies investigating the effect of various PV extracts on different cancer cell lines have been reported in the literature. However, studies on the synthesis of silver NPs from PV extracts and their *in vitro* effects are not available. In this regard, our study will contribute to the literature. In our study, the cytotoxic effects of the synthesized PVAgNPs were found to range from 37.37 to 57.64 µg/mL. We attribute the effectiveness of PVAgNPs at lower doses to the synergy created by PV extracts and nano silver particles.

Table 1: Studies of Plant Extracts for Biosynthesis of Anticancer AgNPs.

Plant	Used part	NP size (nm)	Shape	Cell line	IC_{50} (µg/ml)	References
Phoenix dactylifera	Flowers	27	Irregularly shaped and poly-dispersed	MCF-7	9.06	[74]
Arabian primrose	Leaf	10-60	Spherical	HeLa	7.18	[75]
CAESALPINIA PULCHERRIMA	Leaf	155.4	Spherical	HCT116	3.8	[76]
AZADIRACHTA INDICA	Fruit	27	Spherical	A549	81.09	[77]
PHYCOCYANIN	Pigment	9.39-25.89	Spherical	MCF-7	27.79	[18]
BERGENIA LIGULATA	Whole plant	164.1	Spherical	MCF-7 HCT-116 A549	9.01 11.01 13.06	[78]
CENTELLA ASIATICA	Leaf	20-60	Spherical	MCF-7	8.76	[78]
PEDALIUM MUREX L.	Leaf	11	Spherical	MCF-7	65.60	[79]
CYPERUS CONGLOMERATUS	Root	70-100	Spherical	MCF-7	5.0	[80]
ASIAN SPIDER	*Flower*	20-50	Spherical	MCF-7	40	[81]
PRIMULA VULGARIS	Root *Leaf* *Flower*	40-89	Spherical	MCF-7	36.74 30.37 57.64	This study

A review of the literature revealed that AgNPs have been synthesized in many studies using various plant extracts [18, 74-81]. Most of the AgNPs obtained in these studies are reported to have toxic effects on various cancer cell lines (HeLa, HCT116, A549, MCF-7) or to inhibit growth. The size of the NPs varied between 9.39-164.1 nm according to the studies listed in Table 1. In terms of shape, it is observed that they are mostly spherical. The IC_{50} values of extract-AgNP complexes against MCF-7 cells were between 5.0-65.60 µg/mL. The results of our studies were found to be consistent with the results of previous studies.

CONCLUSION

In conclusion, this study successfully synthesized and characterized PVAgNPs using a green synthesis approach. Characterization of the nanoparticles by various analytical techniques confirmed their cubic crystal structure, stability, predominantly spherical shape, and size range of 40 to 89 nm. In this study, the RTCA system was used, which causes fewer errors than classical methods (MTT, XTT, etc.). The experiments showed that PVAgNPs (leaf, root, and flower extracts) induced cell death in a dose-dependent manner in the MCF-7 cell line. These results highlight the potential of PVAgNPs as targeted drug delivery systems in cancer research. Their unique properties,

combined with the demonstrated efficacy against MCF-7 cells, suggest that PVAgNPs hold promise as novel candidates for the development of future anticancer drugs.

The results suggest that biogenic PVAgNPs offer an alternative approach to overcome several limitations of chemotherapy. However, further research is needed to better understand and elucidate the mechanisms of the cytotoxic effect of PVAgNPs at the molecular level. It is believed that the content of the samples used and the continuation of studies in different cancer cell lines and experimental approaches may pave the way for clinical trials.

ETHICS APPROVAL AND CONSENT TO PARTICIPATE

Not applicable.

HUMAN AND ANIMAL RIGHTS

No animals/humans were used for studies that are the basis of this research.

CONSENT FOR PUBLICATION

Not applicable.

AVAILABILITY OF DATA AND MATERIALS

Not applicable.

FUNDING

None.

CONFLICT OF INTEREST

The authors declare no conflicts of interest, financial or otherwise.

ACKNOWLEDGEMENTS

Declared none.

REFERENCES

[1] McDaniel J. T., Nuhu K., Ruiz J., Alorbi G., Social determinants of cancer incidence and mortality around the world: an ecological study, *Glob. Health Promot.*, **26(1)**: 41-49 (2019).

[2] Siegel R. L., Miller K. D., Jemal A., Cancer statistics, 2018, *CA Cancer J. Clin.*, **68(1)**: 7-30 (2018).

[3] Xu L., Wang Y.-Y., Huang J., Chen C.-Y., Wang Z.-X., Xie H., Silver nanoparticles: Synthesis, medical applications and biosafety, *Theranostics.*, **10(20)**: 8996 (2020).

[4] Shahabi J., Akbarzadeh A., Heydari Nasab A., Ardjmand M., Doxorubicin loaded liposomal nanoparticles containing quantum dot for treatment of breast cancer, *Iran. J. Chem. Chem. Eng. (IJCCE)*, **38(5)**: 45-53 (2019).

[5] da Silva P. B., Machado R. T., Pironi A. M., Alves R. C., De Araújo P. R., Dragalzew A. C., Dalberto I., Chorilli M., Recent advances in the use of metallic nanoparticles with antitumoral action-review, *Curr. Med. Chem.*, **26(12)**: 2108-2146 (2019).

[6] Almatroudi A., Silver nanoparticles: Synthesis, characterisation and biomedical applications, *Open Life Sci.*, **15(1)**: 819-839 (2020).

[7] Kelly K. L., Coronado E., Zhao L. L., Schatz G. C., The optical properties of metal nanoparticles: the influence of size, shape, and dielectric environment. ACS Publications, *J. Phys. Chem. B.*, 2003;107: 668-677 (2006).

[8] Lite M. C., Constantinescu R. R., Tănăsescu E. C., Kuncser A., Romaniţ an C., Lăcătuşu I., Badea N., Design of Green Silver Nanoparticles Based on Primula Officinalis Extract for Textile Preservation, *Materials.*, **15(21)**: 7695 (2022).

[9] Salleh A., Naomi R., Utami N. D., Mohammad A. W., Mahmoudi E., Mustafa N., Fauzi M. B., The potential of silver nanoparticles for antiviral and antibacterial applications: A mechanism of action, *Nanomaterials.* 10(8): 1566 (2020).

[10] Yahya Tahir M., Ahmad A., A. Alothman A., Mushab M. S. S., Ali S., Green Synthesis of Silver Nanoparticles Using Thespesia populnea Bark Extract for Efficient Removal of Methylene Blue (MB) Degradation via Photocatalysis with Antimicrobial Activity and for Anticancer Activity, *Bioinorg. Chem. Appl.*, **2022: 7268273** (2022).

[11] Ratan Z. A., Haidere M. F., Nurunnabi M., Shahriar S. M., Ahammad A. S., Shim Y. Y., Reaney M. J., Cho J. Y., Green chemistry synthesis of silver nanoparticles and their potential anticancer effects, *Cancers.* **12(4)**: 855 (2020).

[12] Sohn E. K., Johari S. A., Kim T. G., Kim J. K., Kim E., Lee J. H., Chung Y. S., Yu I. J., Aquatic toxicity comparison of silver nanoparticles and silver nanowires, *Biomed. Res. Int.*, **2015**: (2015).

[13] Davarnejad R., Azizi A., Asadi S., Mohammadi M., Green synthesis of copper nanoparticles using Centaurea cyanus plant extract: a cationic dye adsorption application, *Iran. J. Chem. Chem. Eng. (IJCCE)*, **41(1)**: 1-14 (2022).

[14] Iravani S., Korbekandi H., Mirmohammadi S. V., Zolfaghari B., Synthesis of silver nanoparticles: chemical, physical and biological methods, *Res. Pharm. Sci.*, **9(6)**: 385 (2014).

[15] Ahmed S., Ahmad M., Swami B. L., Ikram S., A review on plants extract mediated synthesis of silver nanoparticles for antimicrobial applications: a green expertise, *J. Adv. Res.*, **7(1)**: 17-28 (2016).

[16] Hamouda R. A., Hussein M. H., Abo-Elmagd R. A., Bawazir S. S., Synthesis and biological characterization of silver nanoparticles derived from the cyanobacterium Oscillatoria limnetica, *Sci. Rep.*, **9(1)**: 13071 (2019).

[17] Restrepo C. V., Villa C. C., Synthesis of silver nanoparticles, influence of capping agents, and dependence on size and shape: A review, *Environ. Nanotechnol. Monit. Manag.*, **15**: 100428 (2021).

[18] El-Naggar N. E.-A., Hussein M. H., El-Sawah A. A., Bio-fabrication of silver nanoparticles by phycocyanin, characterization, in vitro anticancer activity against breast cancer cell line and in vivo cytotxicity, *Sci. Rep.*, **7(1)**: 10844 (2017).

[19] Venugopal K., Ahmad H., Manikandan E., Arul K. T., Kavitha K., Moodley M., Rajagopal K., Balabhaskar R., Bhaskar M., The impact of anticancer activity upon Beta vulgaris extract mediated biosynthesized

silver nanoparticles (ag-NPs) against human breast (MCF-7), lung (A549) and pharynx (Hep-2) cancer cell lines, *J. Photochem. Photobiol. B: Biol.*, **173**: 99-107 (2017).

[20] Gomathi A., Rajarathinam S. X., Sadiq A. M., Rajeshkumar S., Anticancer activity of silver nanoparticles synthesized using aqueous fruit shell extract of Tamarindus indica on MCF-7 human breast cancer cell line, *J. Drug. Deliv. Sci. Technol.*, **55**: 101376 (2020).

[21] Khan M. A., Khan T., Nadhman A., Applications of plant terpenoids in the synthesis of colloidal silver nanoparticles, *Adv. Colloid Interface. Sci.*, **234**: 132-141 (2016).

[22] Lin Z., Zhou C., Wu J., Zhou J., Wang L., A further insight into the mechanism of Ag^+ biosorption by Lactobacillus sp. strain A09, *Spectrochim. Acta A Mol. Biomol. Spectrosc.*, **61(6)**: 1195-1200 (2005).

[23] Iravani S., Green synthesis of metal nanoparticles using plants, *Green Chem.*, **13(10)**: 2638-2650 (2011).

[24] Mikhailova E. O., Silver nanoparticles: Mechanism of action and probable bio-application, *J. Funct. Biomater.*, **11(4)**: 84 (2020).

[25] Khorrami S., Zarrabi A., Khaleghi M., Danaei M., Mozafari M., Selective cytotoxicity of green synthesized silver nanoparticles against the MCF-7 tumor cell line and their enhanced antioxidant and antimicrobial properties, *Int. J. Nanomedicine.*, 8013-8024 (2018).

[26] Gurunathan S., Qasim M., Park C., Yoo H., Kim J.-H., Hong K., Cytotoxic potential and molecular pathway analysis of silver nanoparticles in human colon cancer cells HCT116, *Int. J. Mol. Sci.*, **19(8)**: 2269 (2018).

[27] Al-Sheddi E. S., Farshori N. N., Al-Oqail M. M., Al-Massarani S. M., Saquib Q., Wahab R., Musarrat J., Al-Khedhairy A. A., Siddiqui M. A., Anticancer potential of green synthesized silver nanoparticles using extract of Nepeta deflersiana against human cervical cancer cells (HeLA), *Bioinorg. Chem. Appl.*, **2018**: (2018).

[28] Yuan Y.-G., Peng Q.-L., Gurunathan S., Silver nanoparticles enhance the apoptotic potential of gemcitabine in human ovarian cancer cells: combination therapy for effective cancer treatment, *Int. J. Nanomedicine.*, 6487-6502 (2017).

[29] Zielinska E., Zauszkiewicz-Pawlak A., Wojcik M., Inkielewicz-Stepniak I., Silver nanoparticles of different sizes induce a mixed type of programmed cell death in human pancreatic ductal adenocarcinoma, *Oncotarget.*, **9(4)**: 4675 (2018).

[30] Fard N. N., Noorbazargan H., Mirzaie A., Hedayati Ch M., Moghimiyan Z., Rahimi A., Biogenic synthesis of AgNPs using Artemisia oliveriana extract and their biological activities for an effective treatment of lung cancer, *Artif. Cells Nanomed. Biotechnol.*, **46(sup3)**: 1047-1058 (2018).

[31] Dawadi S., Katuwal S., Gupta A., Lamichhane U., Thapa R., Jaisi S., Lamichhane G., Bhattarai D. P., Parajuli N., Current research on silver nanoparticles: Synthesis, characterization, and applications, *J. Nanomater.*, **2021**: 1-23 (2021).

[32] Piper J., Charlesworth B., The evolution of distyly in *Primula vulgaris*, *Biol. J. Linn. Soc.*, **29(2)**: 123-137 (1986).

[33] Tütüncü M., In Vitro Culture of Primula: a Review, *J. Agricultural Sci. CFP.*, **13(2)**: 118-125 (2020).

[34] Majd M. T., Asaldoust S., Bahlakeh G., Ramezanzadeh B., Ramezanzadeh M., Green method of carbon steel effective corrosion mitigation in 1 M HCl medium protected by Primula vulgaris flower aqueous extract via experimental, atomic-level MC/MD simulation and electronic-level DFT theoretical elucidation, *J. Mol. Liq.*, **284**: 658-674 (2019).

[35] Woodell S. R., Natural hybridization in Britain between Primula vulgaris Huds (the primrose) and P. elatior (L.) Hill (the oxlip), *Watsonia.*, **7(3)**: 115-112 (1969).

[36] Ozkan M., Aliyazicioglu R., Demir S., Misir S., Turan I., Yildirmis S., Aliyazicioğlu Y., Phenolic characterisation and antioxidant activity of Primula vulgaris and its antigenotoxic effect on fibroblast cells, *Jundishapur J. Nat. Pharm. Prod.*, **12(1)**: (2017).

[37] Obayomi K. S., Lau S. Y., Akubuo-Casmir D., Yahya M. D., Auta M., Bari A. F., Oluwadiya A. E., Obayomi O. V., Rahman M. M., Adsorption of endocrine disruptive congo red onto biosynthesized silver nanoparticles loaded on Hildegardia barteri activated carbon, *J. Mol. Liq*. 352: 118735 (2022).

[38] Wang M., Mo F., Li H., Li Y., Zhang S., Zhu L., Li Z., Xu J., Deng N., Wang K., Adsorption based on weak interaction between phenolic hydroxyl, carboxyl groups and silver nanoparticles in aqueous environment: Experimental and DFT-D3 exploration, *J. Environ. Chem. Eng.*, **9(6)**: 106816 (2021).

[39] Geethalakshmi R., Sarada D. V., Gold and silver nanoparticles from Trianthema decandra: synthesis, characterization, and antimicrobial properties, *Int. J. Nanomed.*, **7**: 5375-5384 (2012).

[40] Gurunathan S., Han J., Park J. H., Kim J. H., A green chemistry approach for synthesizing biocompatible gold nanoparticles, *Nanoscale Res. Lett.*, **9(1)**: 248 (2014).

[41] Wang Z. L., *Transmission electron microscopy and spectroscopy of nanoparticles*. In *Characterization of nanophase materials*, 3: 37-80 (2000).

[42] Ali A., Zafar H., Zia M., Ul Haq I., Phull A. R., Ali J. S., Hussain A., Synthesis, characterization, applications, and challenges of iron oxide nanoparticles, *Nanotechnol. Sci. Appl.*, **9**: 49-67 (2016).

[43] Hunter R. J., *Zeta potential in colloid science: principles and applications*, Academic press: 2013; Vol. 2.

[44] Baskaran X., Geo Vigila A. V., Parimelazhagan T., Muralidhara-Rao D., Zhang S., Biosynthesis, characterization, and evaluation of bioactivities of leaf extract-mediated biocompatible silver nanoparticles from an early tracheophyte, Pteris tripartita Sw, *Int. J. Nanomedicine.*, 5789-5806 (2016).

[45] Joshi N., Jain N., Pathak A., Singh J., Prasad R., Upadhyaya C. P., Biosynthesis of silver nanoparticles using Carissa carandas berries and its potential antibacterial activities, *J Sol-Gel Sci Technol.*, **86**: 682-689 (2018).

[46] Sastry M., Mayya K. S., Bandyopadhyay K., pH Dependent changes in the optical properties of carboxylic acid derivatized silver colloidal particles, *Colloids and Surfaces A: Physicochem. Eng. Asp.*, **127(1-3)**: 221-228 (1997).

[47] Shahverdi A. R., Minaeian S., Shahverdi H. R., Jamalifar H., Nohi A.-A., Rapid synthesis of silver nanoparticles using culture supernatants of Enterobacteria: A novel biological approach, *Process Biochem.*, **42(5)**: 919-923 (2007).

[48] Kelkawi A. H. A., Abbasi Kajani A., Bordbar A. K., Green synthesis of silver nanoparticles using *Mentha pulegium* and investigation of their antibacterial, antifungal and anticancer activity, *IET Nanobiotechnol.*, **11(4)**: 370-376 (2017).

[49] Jang S. J., Yang I. J., Tettey C. O., Kim K. M., Shin H. M., In-vitro anticancer activity of green synthesized silver nanoparticles on MCF-7 human breast cancer cells, *Mater. Sci. Eng. C. Mater. Biol. Appl.*, **68**: 430-435 (2016).

[50] Ashraf H., Anjum T., Riaz S., Naseem S., Microwave-assisted green synthesis and characterization of silver nanoparticles using Melia azedarach for the management of Fusarium wilt in tomato, *Front. Microbiol.*, **11**: 238 (2020).

[51] Rafique M., Sadaf I., Rafique M. S., Tahir M. B., A review on green synthesis of silver nanoparticles and their applications, *Artif. Cells Nanomed. Biotechnol.*, **45(7)**: 1272-1291 (2017).

[52] Urnukhsaikhan E., Bold B.-E., Gunbileg A., Sukhbaatar N., Mishig-Ochir T., Antibacterial activity and characteristics of silver nanoparticles biosynthesized from Carduus crispus, *Sci. Rep.*, **11(1)**: 21047 (2021).

[53] Mostafa F. A., Gamal M. A., Sabrin I. R., Ehab E. S., Antioxidant and anti-inflamatory activities of phenolic constituents from Primula elatior L. aerial part, *Int. J. Pharmacogn. Phytochem.*, **6(1)**: 74-78 (2014).

[54] Mourdikoudis S., Pallares R. M., Thanh N. T., Characterization techniques for nanoparticles: comparison and complementarity upon studying nanoparticle properties, *Nanoscale.*, **10(27)**: 12871-12934 (2018).

[55] Sathyavathi R., Krishna M. B., Rao S. V., Saritha R., Rao D. N., Biosynthesis of Silver Nanoparticles Using *Coriandrum Sativum* Leaf Extract and Their Application in Nonlinear Optics, *Adv. Sci. Lett.*, **3(2)**: 138-143 (2010).

[56] Philip D., *Mangifera indica* leaf-assisted biosynthesis of well-dispersed silver nanoparticles, *Spectrochim. Acta. A Mol. Biomol. Spectrosc.*, **78(1)**: 327-331 (2011).

[57] Nindawat S., Agrawal V., *Arabian Primrose* leaf extract mediated synthesis of silver nanoparticles: their industrial and biomedical applications, *Artif. Cells Nanomed. Biotechnol.*, **48(1)**: 1259-1271 (2020).

[58] Ramar M., Manikandan B., Marimuthu P. N., Raman T., Mahalingam A., Subramanian P., Karthick S., Munusamy A., Synthesis of silver nanoparticles using *Solanum trilobatum fruits* extract and its antibacterial, cytotoxic activity against human breast cancer cell line MCF 7, *Spectrochim. Acta. A Mol. Biomol. Spectrosc.*, **140**: 223-228 (2015).

[59] Vivek R., Thangam R., Muthuchelian K., Gunasekaran P., Kaveri K., Kannan S., Green biosynthesis of silver nanoparticles from *Annona squamosa* leaf extract and its in vitro cytotoxic effect on MCF-7 cells, *Process. Biochem.*, **47(12)**: 2405-2410 (2012).

[60] Devanesan S., AlSalhi M. S., Green synthesis of silver nanoparticles using the flower extract of Abelmoschus esculentus for cytotoxicity and antimicrobial studies, *Int. J. Nanomedicine.*, 3343-3356 (2021).

[61] Dhar S. A., Chowdhury R. A., Das S., Nahian M. K., Islam D., Gafur M. A., Plant-mediated green synthesis and characterization of silver nanoparticles using Phyllanthus emblica fruit extract, *Materials Today: Proceedings.*, **42**: 1867-1871 (2021).

[62] Logeswari P., Silambarasan S., Abraham J., Synthesis of silver nanoparticles using plants extract and analysis of their antimicrobial property, *J. Saudi Chem. Soc.*, **19(3)**: 311-317 (2015).

[63] Rani P., Kumar N., Perinmbam K., Devanesan S., AlSalhi M. S., Asemi N., Nicoletti M., Synthesis of Silver Nanoparticles by Leaf Extract of *Cucumis melo* L. and Their In Vitro Antidiabetic and Anticoccidial Activities, *Molecules.*, **28(13)**: 4995 (2023).

[64] Patil S., Sandberg A., Heckert E., Self W., Seal S., Protein adsorption and cellular uptake of cerium oxide nanoparticles as a function of zeta potential, *Biomater.*, **28(31)**: 4600-4607 (2007).

[65] Xu R., Progress in nanoparticles characterization: Sizing and zeta potential measurement, *Particuology.*, **6(2)**: 112-115 (2008).

[66] Jiang J., Oberdörster G., Biswas P., Characterization of size, surface charge, and agglomeration state of nanoparticle dispersions for toxicological studies, *J. Nanopart. Res.*, **11**: 77-89 (2009).

[67] Turan İ., Demir S., Aliyazıcıoğlu R., Aliyazıcıoğlu Y., Evaluation of antioxidant and cytotoxic properties of *Primula vulgaris* leaf extract, *KSU J. Nat. Sci.*, **20(4)**: 361-367 (2017).

[68] Hu M. L., Dietary polyphenols as antioxidants and anticancer agents: more questions than answers, *Chang. Gung. Med. J.*, **34(5)**: 449-460 (2011).

[69] Shostak L., Marchyshyn S., Kozachok S., Karbovska R., Investigation of phenolic compounds of Primula veris L, *J. Educ. Health Sport.*, **6(5)**: 424-432 (2016).

[70] Ravishankar D., Rajora A. K., Greco F., Osborn H. M., Flavonoids as prospective compounds for anti-cancer therapy, *Int. J. Biochem. Cell Biol.*, **45(12)**: 2821-2831 (2013).

[71] Zhou Y., Zheng J., Li Y., Xu D. P., Li S., Chen Y. M., Li H. B., Natural Polyphenols for Prevention and Treatment of Cancer, *Nutrients.*, **8(8)**: (2016).

[72] Demir S., Turan İ., Aliyazıcıoğlu Y., Antioxidant properties of *Primula vulgaris* flower extract and its cytotoxic effect on human cancer cell lines, *KSU J. Agric. Nat.*, **22(1)**: 78-84 (2019).

[73] Demir S., Turan I., Aliyazicioglu R., Yaman S. O., Aliyazicioglu Y., *Primula vulgaris* extract induces cell cycle arrest and apoptosis in human cervix cancer cells, *J. Pharm. Anal.*, **8(5)**: 307-311 (2018).

[74] Banu H., Renuka N., Faheem S., Ismail R., Singh V., Saadatmand Z., Khan S. S., Narayanan K., Raheem A., Premkumar K., Gold and silver nanoparticles biomimetically synthesized using date palm pollen extract-induce apoptosis and regulate p53 and Bcl-2 expression in human breast adenocarcinoma cells, *Biol.Trace Elem. Res.*, **186**: 122-134 (2018).

[75] Nindawat S., Agrawal V., Arabian Primrose leaf extract mediated synthesis of silver nanoparticles: their industrial and biomedical applications, *Artif. Cells Nanomed. Biotechnol.*, **48(1)**: 1259-1271 (2020).

[76] Deepika S., Selvaraj C. I., Roopan S. M., Screening bioactivities of Caesalpinia pulcherrima L. swartz and cytotoxicity of extract synthesized silver nanoparticles on HCT116 cell line, *Mater. Sci. Eng. C.*, **106**: 110279 (2020).

[77] Alharbi N. S., Alsubhi N. S., Green synthesis and anticancer activity of silver nanoparticles prepared using fruit extract of Azadirachta indica, *J. Radiat. Res. Appl. Sci.*, **15(3)**: 335-345 (2022).

[78] Faheem M. M., Bhagat M., Sharma P., Anand R., Induction of p53 mediated mitochondrial apoptosis and cell cycle arrest in human breast cancer cells by plant mediated synthesis of silver nanoparticles from Bergenia ligulata (Whole plant), *Int. J. Pharm.*, **619**: 121710 (2022).

[79] Balan L., Chandrasekaran S., Gajendiran M., Nanjian R., Synthesis of silver nanoparticles from Pedalium murex L. and its antiproliferative activity against breast cancer (MCF-7) cells, *J. Mol. Struct.*, **1242**: 130695 (2021).

[80] Al-Nuairi A. G., Mosa K. A., Mohammad M. G., El-Keblawy A., Soliman S., Alawadhi H., Biosynthesis, characterization, and evaluation of the cytotoxic effects of biologically synthesized silver nanoparticles from cyperus conglomeratus root extracts on breast cancer cell line MCF-7, *Biol. Trace Elem. Res.*, **194**: 560-569 (2020).

[81] Pannerselvam B., Durai P., Thiyagarajan D., Song H. J., Kim K. J., Jung Y. S., Kim H. J., Rangarajulu S. K., Facile synthesis of silver nanoparticles using Asian spider flower and its in vitro cytotoxic activity against human breast carcinoma cells, *Processes.*, **8(4)**: 430 (2020).